Int. J. Electrochem. Sci., 9 **(2014)** 2682 - 2695

International Journal of
ELECTROCHEMICAL
SCIENCE
www.electrochemsci.org

The Effect of Solution pH of Permanganate Coating on the Electrochemical Characteristics of ZE41 Magnesium Alloy in Chloride Media

Abdel Salam Hamdy[*] *and H. M. Hussien*

Central Metallurgical Research and Development Institute, P.O. Box: 87, Helwan, 11421 Cairo, Egypt.
[*]E-mail: asalam85@yahoo.com

Received: 23 July 2013 / *Accepted:* 2 February 2014 / *Published:* 2 March 2014

Replacement of heavy alloys components with light-weight materials has been of prime concern for automotive and aerospace manufactures during the last decade. The main driving force behind such direction is to reduce the fuel consumption and hence polluted CO_2 emission. ZE41 is one of the magnesium alloys that was proposed for this function owing to its promising mechanical performance. However, the high corrosion susceptibility is the main reason that limits spreading such alloy in industry. This paper provides a deep investigation on the electrochemical characteristics and morphology of the film formed as a function of Mn-coating pHs in order to optimize the coating conditions. Results confirmed that the optimum coating pH is 7.5. Changing the coating pH around 7.5 has a detrimental effect on the localized corrosion resistance.

Keywords: permanganate treatment, ZE41 Mg-Zn-rare earth alloy, clean protective coatings, corrosion.

1. INTRODUCTION

Magnesium alloys have been proposed for automotive, electronics and aircraft industries owing to their attractive physical and mechanical properties, such as high thermal and electrical conductivities, low density, stiffness, mechanical stability, good vibration and shock absorption ability. Unfortunately, the very high corrosion susceptibility of magnesium is the main challenge that limits using these alloys in industrial applications.

Many attempts have been invested to improve the corrosion resistance of Mg alloys. Some schemes have, indeed, been proposed, for example, changing the chemical composition of the alloys through addition of some rare-earth elements such as Zr, Ce, Nd,..etc (example is the alloy under

investigation in this paper), surface modification treatments prior to applying the coating, or the use of protective films and coatings.

Coating was proved to be the most effective way to improve the corrosion resistance of magnesium. Several coating technologies are currently in use to provide adequate corrosion protection for magnesium alloys [1-46]. These include the electro- and electroless plating, conversion coatings, anodizing, hydride coatings, organic coatings and CVD and PVD. However, chemical surface treatments have proven to effectively improve the corrosion resistance of Mg alloys include anodising treatments and chemical conversion-coating treatments.

The most effective process considering the feasibility issues for possible scaling-up in industrial application is the conversion coating technique. Chemical conversion coating have been extensively used for improving the corrosion resistance of magnesium alloys [3-46].

Chromate baths containing hexavalent chromium compounds have been the most common industrial conversion coatings for steel, aluminum and magnesium alloys. Chromium conversion coating was the best ever during the last century to produce smart protective films with self-healing functionalities. However, chromate conversion coatings are now being banned due to their toxicity and carcinogenic effect. Accordingly, that triggered intensive research from industry and academia on the preparation of chrome-free coatings.

Chrome-free eco-friendly conversion coatings for magnesium alloys have thus received ever-increasing attention during the last decade, including environmentally acceptable salts of zirconate, vanadate, stannate, rare-earth metal salt, phosphate, titanate, and phosphate/permanganate conversion coatings [3-46]. Despite the intensive research efforts invested to optimize a chrome-free coating technology on magnesium alloys, the problem of replacement toxic chromate has not been resolved yet and, it is unfortunate that the toxic chromate are still used in the industry.

Most, if not all, of the published data about permanganate conversion coatings are based on multi-step coating layers or surface treatments followed by a post-treatment in phosphate solution which makes the overall process quite unattractive [23-36, 41-45]. In this paper, the permanganate conversion coatings on magnesium ZE41 Mg-Zn-rare earth alloy were prepared using free immersion method in permanganate baths differing in pHs. The optimum permanganate coating bath concentration that can offer the best corrosion resistance to magnesium ZE41 Mg-Zn-rare earth alloy has been determined in a previous study to be 10 g/l [37]. The corrosion behavior of as-abraded and permanganate coated magnesium ZE41 Mg-Zn-rare earth alloy has been investigated by electrochemical impedance spectroscopy, cyclic voltammetry and linear polarization methods. The effect of changing the pH of the bath composition at pH values 5.5, 7.5, and 9.5 on the corrosion resistance of the coated alloy has been evaluated. Changing the morphology and chemical composition of the films formed as a result of changing the pH were investigated by the scanning electron microscopy (SEM-EDS) and X-ray diffraction (XRD) techniques and compared with the corrosion resistance of the as-abraded samples.

2. EXPERIMENTAL

2.1. Materials and surface preparation

Specimens of Elektron ZE41 in the form 30 x 60 x 3mm were cut from a sand cast plate 100 x 200 x 25mm provided by Magnesium Elektron, UK. The alloy chemical composition and the specimens preparation were given in details elsewhere [37].

2.2. Solutions and surface treatment

The bath formulation of permanganate coatings investigated in this study are formed from aqueous solutions containing 10 g/l of $KMnO_4$ using a free immersion processing technology that is very similar to that currently used for the toxic chromate system. A thin layer of manganese oxide conversion coatings is deposited on the magnesium alloy surface. Depositions are achieved in 10 minutes and use commercially available chemical and equipment, making the overall process compatible with industrial operations such as those employed by current aircraft manufacturers.

Solutions used in this work were prepared using potassium permanganate salt with different pHs. The ZE41 substrates were treated directly by simple free immersion in permanganate solutions at different pHs namely 5.5, 7.5, and 9.5 solutions for 10 minutes at room temperature. As-abraded samples (uncoated) were used as a blank.

2.3. Testing

The experimental setting for electrochemical impedance spectroscopy, linear polarization, and cyclic voltammetry measurements has been provided in details elsewhere [37]. The surface characterization conditions and instrumentations have been also provided in [37].

3. RESULTS AND DISCUSSION

The corrosion resistance of permanganate coated ZE41 Mg-Zn-rare earth alloy was investigated in views of the optimum permanganate solution pHs that can provide the highest corrosion resistance to Mg substrate. Our previous results showed that the optimum permanganate concentration which can offer the best corrosion resistance to Mg substrate is 10 g/l [37].

In this paper we are attempting to optimize the permanganate coating pHs as a function of the corrosion inhibition characteristics of ZE41 Mg-Zn-rare earth alloy in NaCl solution. Consequently, we will use the optimum permanganate solution concentration (10 g/l) determined in the previous studies [37] as a base for determining the optimum pH.

3.1. Visual inspection and macroscopic examination

Macroscopic images of as-abraded ZE41 Mg-Zn-rare earth alloy panels showed severe localized (pitting and crevice) corrosion attack after one week of immersion in 3.5% NaCl solution (Fig. 1). Permanganate coated panels revealed formation of a Mn rich magnesium hydroxide film over the magnesium substrate. After one week of immersion in corrosive NaCl solution, the samples coated with permanganate at pH 5.5 and 9.5 showed severe pitting and crevice corrosion close to the behavior

of as-abraded sample. Conversely, the samples coated with permanganate at pH 7.5 showed the best corrosion protection. Only few tiny pits with limited areas of crevice corrosion were observed (Fig. 1).

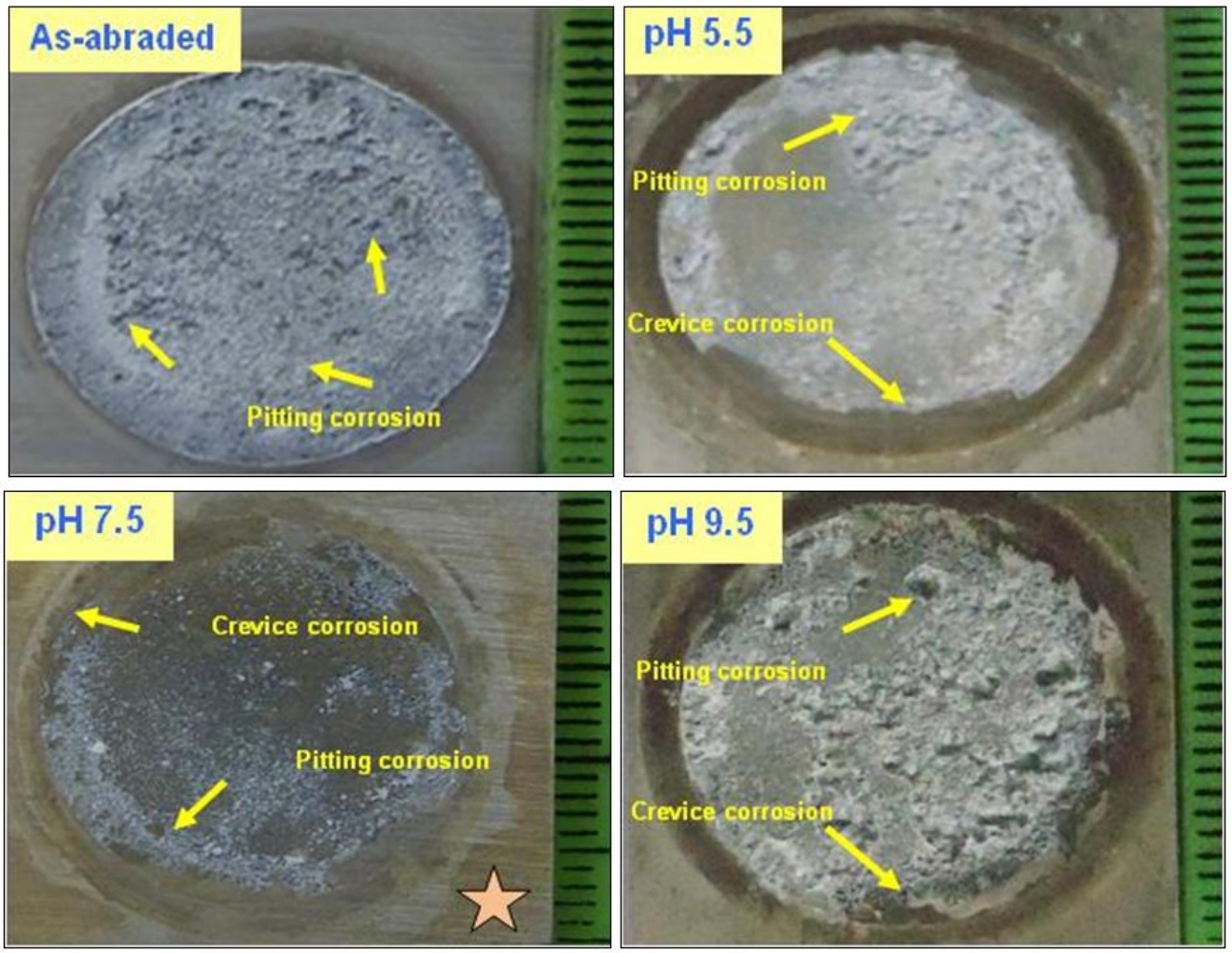

Figure 1. Macroscopic images show the effect of changing the permanganate coating pH on the corrosion resistance of ZE41 Mg-Zn-rare earth alloy after seven days of immersion in 3.5 % NaCl solution. As-abraded samples show pitting and crevice corrosion. pH 7.5 offers the best corrosion resistance.

3.2. Pitting corrosion density

A comparison between the pitting corrosion density of the as-abraded and permanganate coated samples at different pHs has been investigated. The average pitting density as calculated by visual inspection and microscopic examination after seven days of immersion in 3.5% NaCl solution is given in Fig. 2. Results showed that the high pitting susceptibility can be sorted in the following order: pH 9.5 > as-abraded > pH 5.5 > pH 7.5. Accordingly, the film formed due to permanganate coating at pH 7.5 is the best to offer acceptable localized corrosion resistance to Mg substrate. Changing the neutral

pH of permanganate coating (pH 7.5) towards acidic (pH 5.5) or alkaline (pH 9.5) enhances the formation of less protective films.

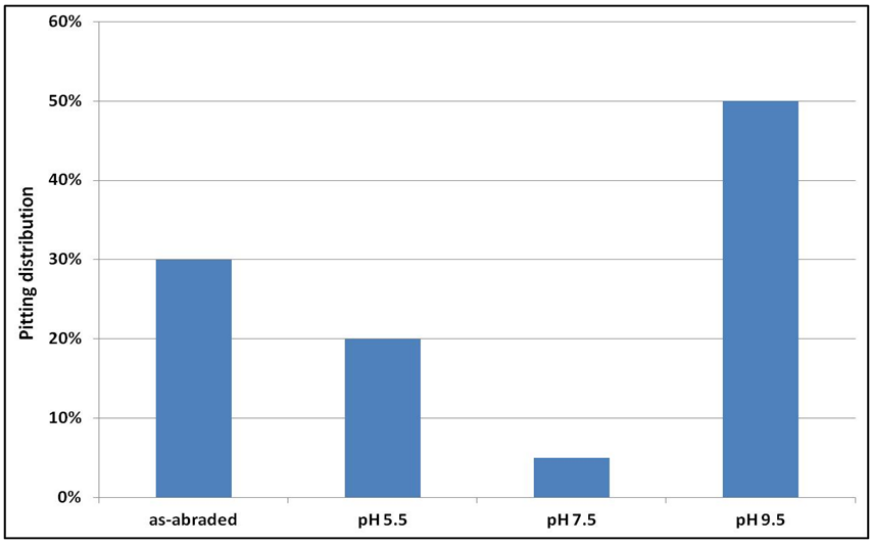

Figure 2. Pitting corrosion density of as-abraded and permanganate coated samples at different pHs after one week of immersion in NaCl solution

Decreasing the passivity due to changing the pHs either towards acidic or alkaline values can be attributed to the changes in the chemical composition of the film formed. The next section (3.3) discusses in details the possibility of changing the chemical composition as a function of pH using Pourbaix diagram.

3.3. X-ray diffractometry (XRD)

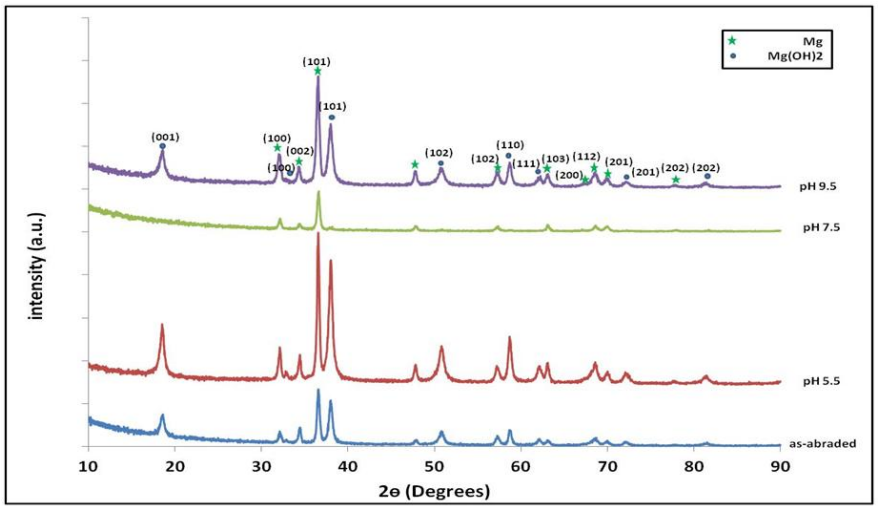

Figure 3. XRD analysis of the corrosion products formed at permanganate coated samples after immersion in NaCl solution

XRD analyses of the corrosion products formed over the as-abraded and permanganate coated samples are given in Fig. 3. Generally, no manganese peaks were identified. That may be due to formation a very thin-film of Mn at the Mg substrate which is out of the accuracy limits of the XRD instrument. However, XRD spectra of the corrosion products formed at pH 7.5 revealed presence of Mg as a metal while other coated samples at pH 5.5 or 9.5 revealed formation of magnesium hydroxide $Mg(OH)_2$.

Pourbaix diagram (Fig. 4) and the colors examination of the films formed in Fig. 1 provides an explanation for improving the stability of the dark brown film (Mn_2O_3) formed at pH 7.5. Mn_2O_3 is a strong oxidizing agent and thermodynamically more stable (and theoretically more abundant) than the other films formed at different pH conditions under investigation. Indeed, this finding provides better understanding about the chemistry behind the presence of Mg metal in case of the samples coated at pH 7.5 and magnesium hydroxide $Mg(OH)_2$ in the other samples coated.

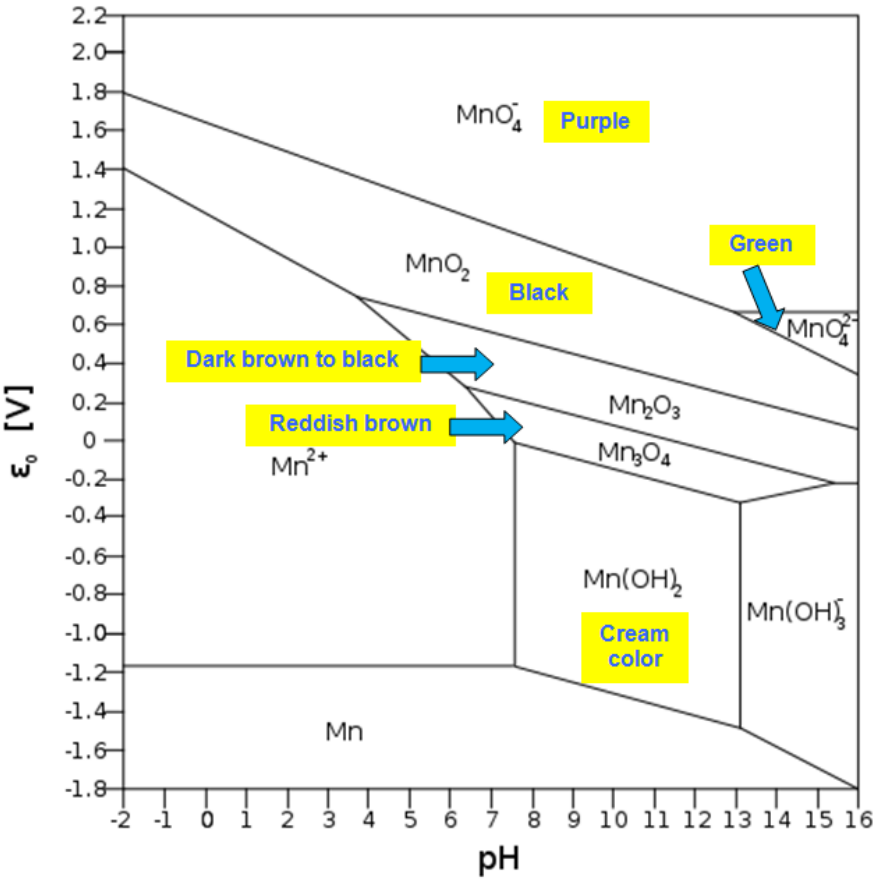

Figure 4. Pourbaix diagram for the Mn-O-H system (the area between the two diagonal lines from the upper left to the lower right in the diagram indicates the stability field of water at 298.15 k and 10^5 Pa. total concentration of elements is 10^{-10} mole/kg.)

3.4. Corrosion tests

A series of electrochemical experiments was performed on as-abraded and permanganate coated ZE41 Mg-Zn-rare earth alloy panels in corrosive chloride medium in order to determine the

optimum pH conditions for improving the localized corrosion resistance and, consequently, to investigate potential protective coating for such promising material in order to spread its use in industry.

3.4.1. Electrochemical impedance spectroscopy

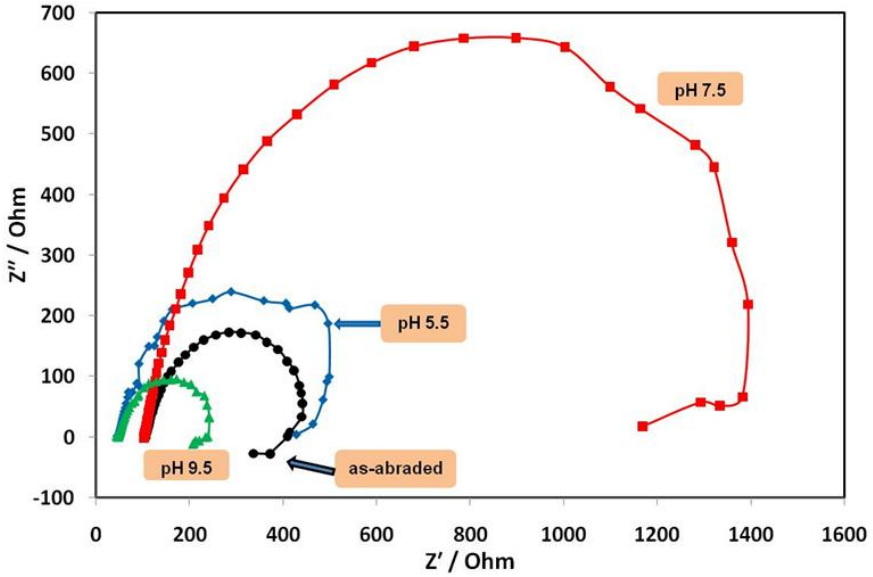

Figure 5. Nyquist plots for as-abraded and permanganate coated magnesium samples at different pHs after one week of immersion in 3.5 %NaCl solution

The corrosion resistance of as-abraded and permanganate coated ZE41 Mg-Zn-rare earth alloy panels at pH 5.5, 7.5 and 9.5 were investigated in corrosive 3.5% NaCl solution. According to Nyquist plots (Fig. 5), the best resistance and capacitance values were obtained for the panels coated with permanganate at pH 7.5. The surface resistance of the samples coated with permanganate solution at pH 7.5 is almost three times larger than the resistance of the sample coated with permanganate at pH 5.5 and six times larger than the resistance of the sample coated with permanganate at pH 9.5. The measured surface resistances can be sorted in the following order 1.40×10^3 $\Omega.cm^2$, 0.50×10^3 $\Omega.cm^2$, 0.41×10^3 $\Omega.cm^2$, and 0.25×10^3 $\Omega.cm^2$ for pH 7.5, pH 5.5, as-abraded, and pH 9.5 respectively. This preliminary result allows conditions to be established for optimization of the pH of permanganate coatings for improving the corrosion protection of ZE41 Mg-Zn-rare earth alloy in corrosive chloride solutions.

3.4.2. Polarization measurements

The stability of the film formed on ZE41 Mg-Zn-rare earth alloy panels after permanganate coatings at pH 5.5, 7.5 and 9.5 was evaluated in a 3.5% NaCl solution. The resultant coatings at pH 7.5, tested in the presence of aggressive chloride ions, revealed a shift towards more passive current when compared with other samples coated at pH 5.5 and 9.5 as shown in Table 1 and Fig. 6.

Moreover, the lowest corrosion rate (C.R.) values were obtained from the permanganate coated samples at pH 7.5 (Table 1). The value of corrosion rate was ~ 0.02 mm/y which is lower than the values obtained from samples coated at pH 9.5, equals to 1/3 of the values obtained from samples coated at pH 5.5 and 1/10 the as-abraded panels (Table 1).

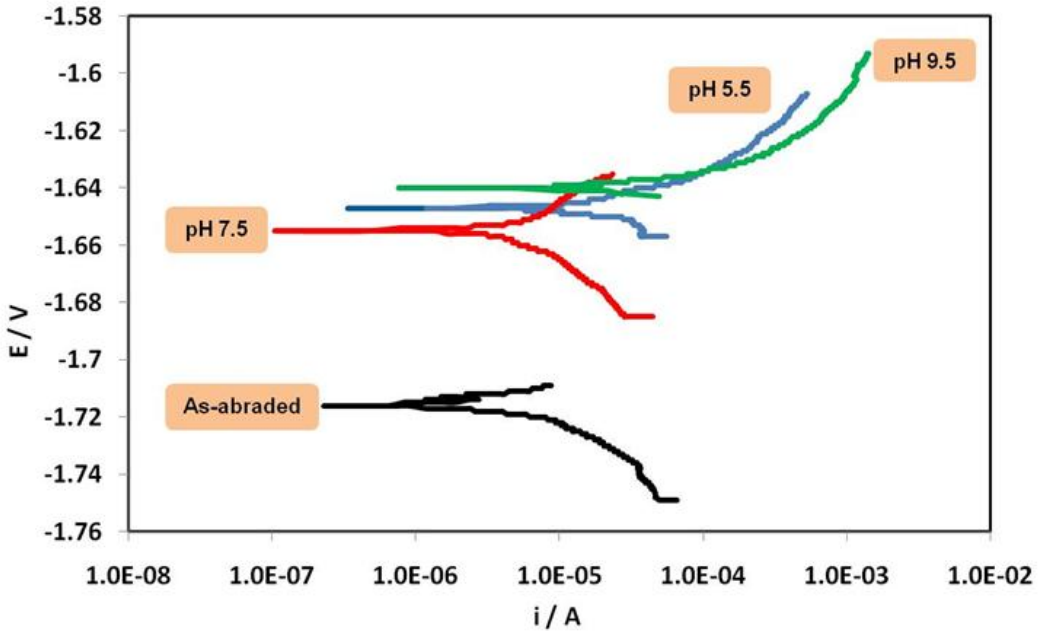

Figure 6. Linear polarization for as-abraded and permanganate coated magnesium samples at different pHs after 30 minutes of immersion in 3.5 %NaCl solution

Table 1. Polarization data for as-abraded and permanganate coated magnesium samples at different pHs after 30 minutes of immersion in 3.5 %NaCl solution

	Rp (Ohm)	E Corr (V)	I Corr (A/cm^2)	C.R. (mm/year)
As-abraded	14.98	-1.729	$5.324*10^{-7}$	$58.07*10^{-2}$
PH 5.5	11.81	-1.646	$8.439*10^{-6}$	$6.32*10^{-2}$
PH 7.5	92.27	-1.655	$4.562*10^{-6}$	$1.96*10^{-2}$
PH 9.5	44.02	-1.641	$2.963*10^{-6}$	$2.22*10^{-2}$

The polarization resistance (Rp) of the permanganate coated panels at pH 7.5 was measured to be 92.27 Ω which is more than double of the panels coated at pH 9.5, nine times of the panels coated at pH 5.5, and approximately eight times of the as-abraded panels (Fig. 6 and Table 1).

It is clearly apparent that the corrosion current density and corrosion rate are changed significantly with changing the permanganate coating pHs. The ZE41 Mg-Zn-rare earth alloy panels coated with permanganate at pH 7.5 showed the highest current density and lowest corrosion rate. In

addition, the limiting current of the ZE41 Mg-Zn-rare earth alloy panels coated with permanganate at pH 7.5 showed a significant shift towards the negative (more passive) direction compared to the other samples. These results provide another evidence that that treatment at pH 7.5 offers the best corrosion resistance.

3.4.3. Cyclic voltammetry (CV) measurements

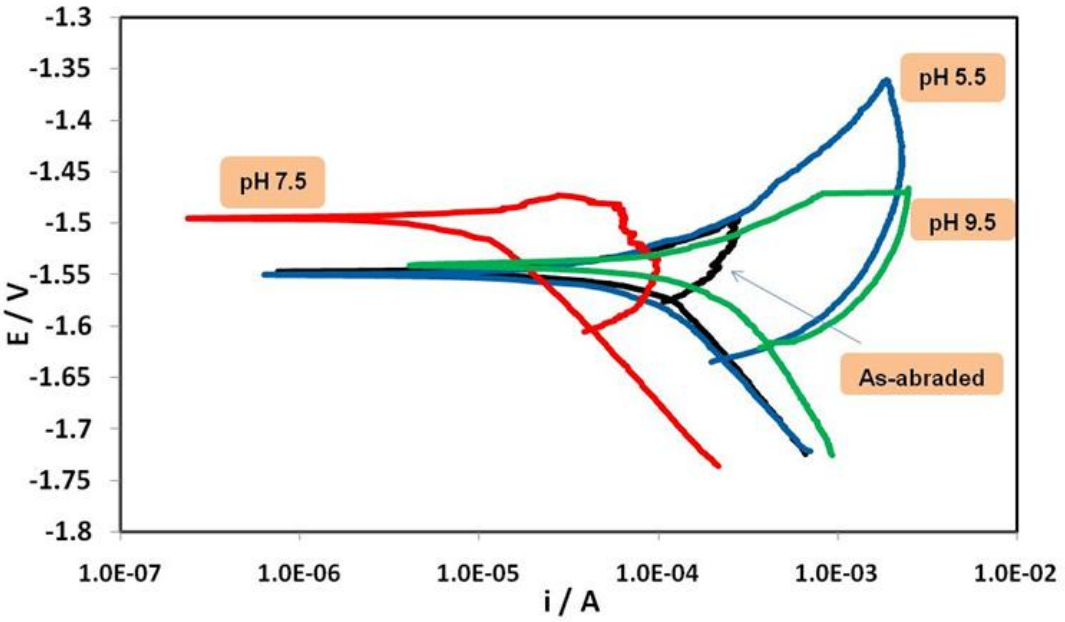

Figure 7. Cyclic voltammetry for as-abraded and permanganate coated magnesium samples at different pHs after one week of immersion in 3.5 %NaCl solution

The influence of changing the permanganate coating pH on the pitting corrosion behavior of ZE41 Mg-Zn-rare earth alloy panels was studied in 3.5% NaCl solutions. Cyclic potentiodynamic technique (Fig. 7) was used to evaluate the pitting corrosion resistance after one week of immersion in NaCl solution. The importance of this technique and its validity to provide a clear-cut about the pitting corrosion behavior have been discussed elsewhere [39, 40, 46].

Results showed that the pitting area under the loop, which represents the chance of pitting corrosion to occur; of the permanganate coated panels at pH 7.5 is smaller than the other coated samples at pH 5.5 and 9.5. That finding is in agreement with the other results obtained from EIS, linear polarization, calculated pitting corrosion density, maco- and micro-images.

Surprisingly, the area under the loop of the as-abraded samples is relatively smaller than that obtained from the permanganate coated panels at pH 7.5 (Fig. 7). This result doesn't match with the pitting corrosion density data calculated in Fig. 2 and the impedance spectra in Fig. 5 where the measured surface resistance of permanganate coated panels at pH 7.5 was 1.40×10^3 $\Omega.cm^2$ which is about four times the value of as-abraded samples 0.41×10^3 $\Omega.cm^2$.

The apparent disagreement between the EIS (Fig. 5) and the pitting corrosion density data calculated in Fig. 2 from one hand; and the CV results (Fig. 7) from the other hand, can be explained

by the fact that the measured surface resistance by EIS expresses the total surface resistance including the pitting, crevice, and general corrosion while CV data represents the pitting corrosion only. In fact, the sharp potential difference between the rare-earth-metals phase formed (Fig. 8 left) in ZE41 Mg-Zn-rare earth alloy (acts as cathode) and the surrounding Mg matrix (acts as anode) results in originating an electrochemical cell and enhancing the galvanic corrosion at the interfaces. Increasing the immersion time of ZE41 Mg-Zn-rare earth alloy in corrosive NaCl solution, results in debonding of the inert cathodic phase of rare-earth elements which can be dropped from the matrix leaving a hole (Fig. 8 right).

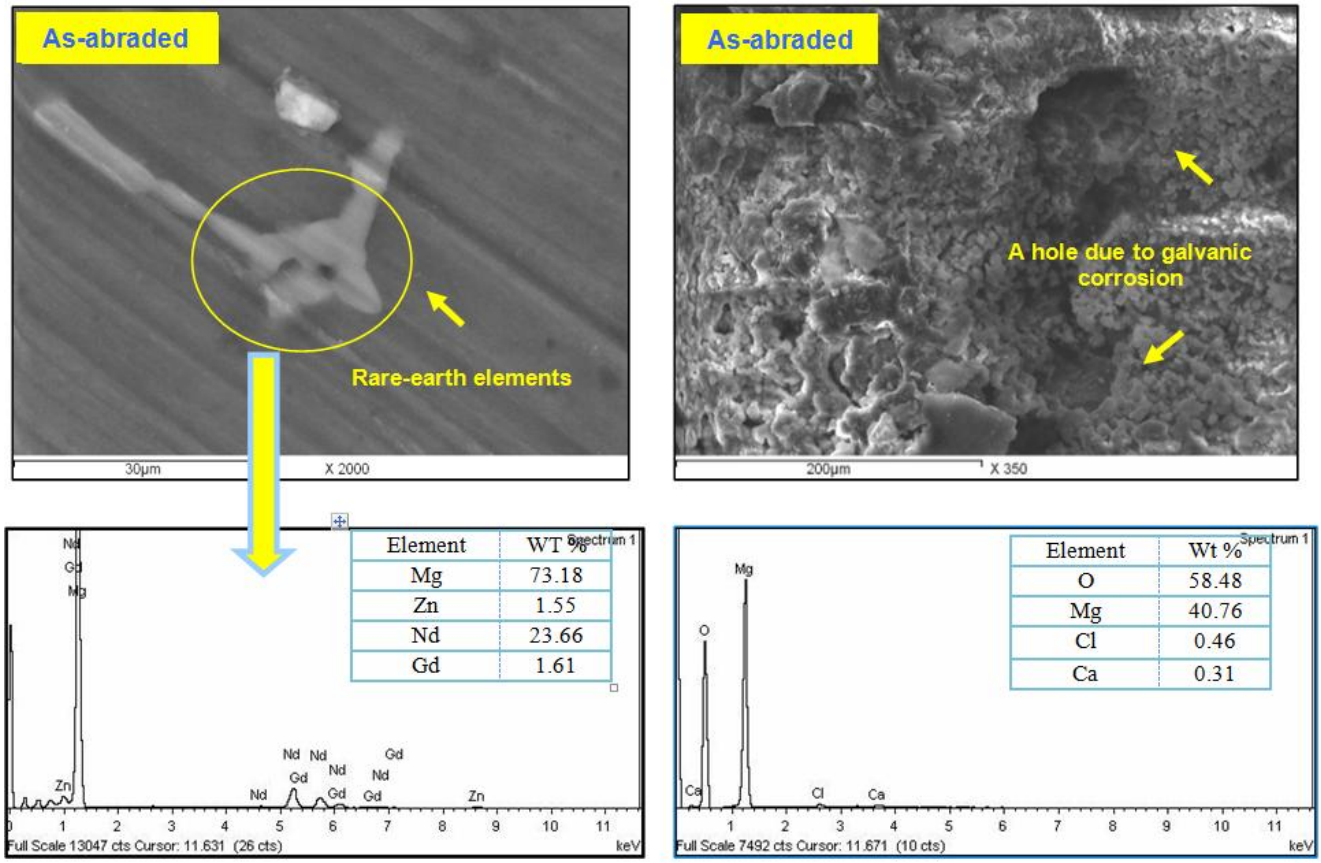

Figure 8. SEM-EDS of as-abraded ZE41 Mg-Zn-rare earth alloy panels before (left) and after (right) corrosion. The images focus on the formation of rare-earth elements phase in a Mg matrix and the possible galvanic corrosion at the interfaces

3.5. Microscopic examination using SEM-EDS

SEM micrograph of the as-abraded samples before corrosion (Fig. 8) revealed presence of a rare-earth metals phase in the Mg matrix as explained above. After one week of exposure to NaCl solution, severe localized corrosion has been identified as shown in Fig. 8. SEM indicated that galvanic corrosion initiated at the interface between the rare-earth metals phase and the Mg matrix in addition to pitting corrosion.

Changing the surface morphology of ZE41 Mg-Zn-rare earth alloy after applying permanganate coatings at different pHs is illustrated in Figs. 9, 10, and 11. Generally, a permanganate thin-film was formed at Mg surface. However, the film formed due to permanganate coating at pH 7.5 has a much better surface distribution and almost free from the coating defects compared to the other coated samples that showed some surface defects through them localized corrosion can occur (Figs. 9, 10, 11).

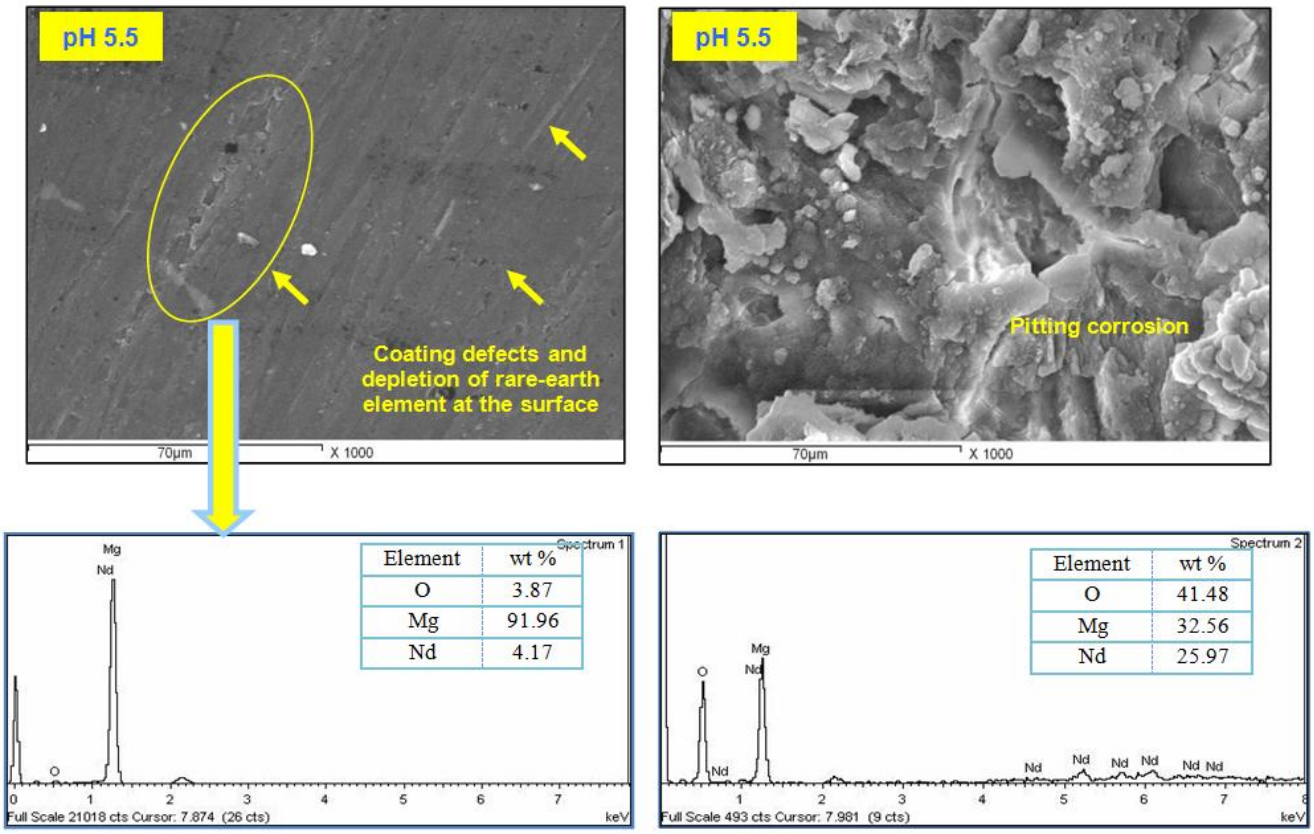

Figure 9. SEM-EDS of permanganate coated ZE41 Mg-Zn-rare earth alloy panels at pH 5.5 before (left) and after (right) corrosion. The images focus on the formation of a thin Mn-coating with some defects and occurrence of pitting corrosion

The presence of few pitting zones in the permanganate coated panels at pH 7.5 can be attributed to formation of very thin Mn-rich film formed (XRD in Fig. 3 was not able to detect the presence of Mn due to the accuracy limits). This film behaves as barrier to protect the material substrate from the reaction with dissolved oxygen in Cl^- solution and hence impedes the localized corrosion by shifting the cathodic reaction to more noble current (Figs. 6, 7 and Table 1). This result supports the idea of formation of a stable dark brown film (Mn_2O_3) which is a strong oxidizing agent and thermodynamically more stable (and theoretically more abundant) than the other films formed (Fig. 4).

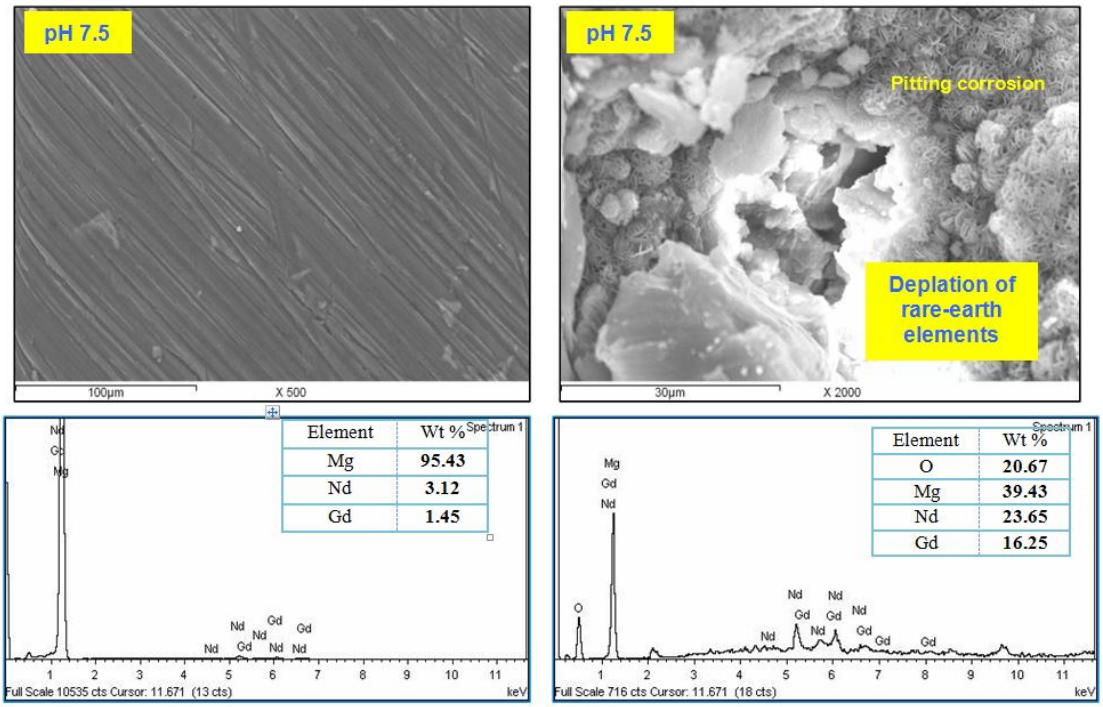

Figure 10. SEM-EDS of permanganate coated ZE41 Mg-Zn-rare earth alloy panels at pH 7.5 before (left) and after (right) corrosion. The images focus on the formation od uniform and smooth Mn-thin film and an example of a tiny pit.

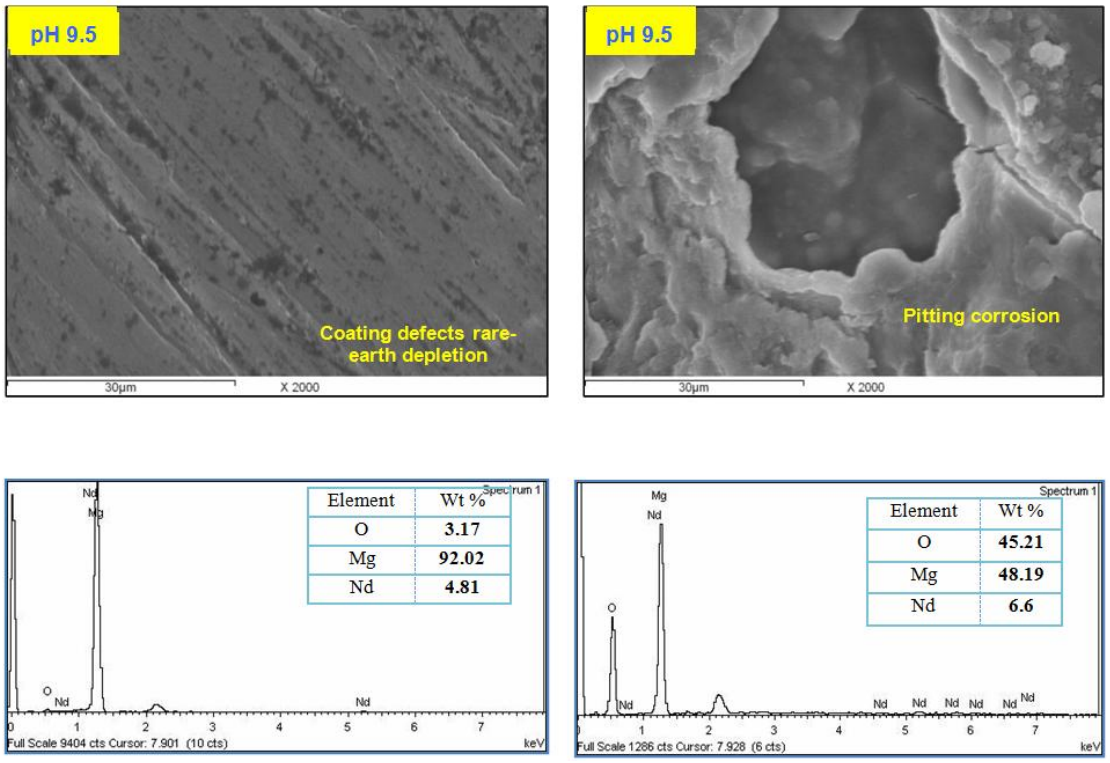

Figure 11. SEM-EDS of permanganate coated ZE41 Mg-Zn-rare earth alloy panels at pH 9.5 before (left) and after (right) corrosion. The images focus on the formation of a thin-film of permanganate with many surface defects and an example of pitting corrosion.

4. CONCLUSION

1- Alloying with rare earth elements enhances the galvanic corrosion and decrease the overall corrosion resistance of Mg alloys.

2- The optimum permanganate solution pH was found to be pH 7.5 (neutral solution pH) which has proven to offer the best localized corrosion resistance upon immersion in chloride containing environments.

3- The importance of this study is that it provides a simple coating technology for improving the corrosion resistance of ZE41 Mg-Zn-rare earth alloy panels in corrosive chloride medium. Finding a potential protective coating technology for such promising magnesium alloy will help the manufactures to spread its application in industry.

References

1. A.S. Hamdy and I. Tiginyanu (Editors), “Nanocoatings and Ultra Thin-Films”, Woodhead Publishing Limited, UK, ISBN: 978-1-84569-812-6, 2011.
2. A.S. Hamdy (Editor): “Handbook of Smart Coatings for Corrosion Protection”, Woodhead Publishing Limited, UK, in press 2013. http://www.woodheadpublishing.com/en/book.aspx?bookID=2745
3. M.A. Gonzalez-Nunez, P. Skeldon, G.E. Thompson, H. Karimzadeh, *Corrosion* 55 (1999) 1136–1143.
4. C.S. Lin, H.C. Lin, K.M. Lin, W.C. Lai, *Corros. Sci.* 48 (2006) 93–109.
5. A.S. Hamdy (Editor): "High Performance Coatings for Automotive and Aerospace Industries”, Nova Science Publishers, NY, USA, ISBN: 978-1-60876-579-9, 2010.
6. L. Rudd, C.B. Breslin, F. Mansfeld, *Corros. Sci.* 42 (2000) 275–288.
7. M. Dabalà, K. Brunelli, E. Napolitani, M. Magrini, *Surf. Coat. Technol*. 172 (2003) 227–232.
8. K. Brunelli, M. Dabalà, I. Calliari, M. Magrini, *Corros. Sci.* 47 (2005) 989–1000.
9. C.S. Lin, S.K. Fang, *J. Electrochem. Soc.* 152 (2005) B54–B59.
10. C.S. Lin, W.J. Li, *Mater. Trans*. 47 (2006) 1020–1025.
11. A. S. Hamdy, *Anti-Corros Methods Mater.*, 53, 6 (2006) 367–373
12. A.S. Hamdy, *Electrochem Solid St*., 10, 3, (2007) C21-C25.
13. A.S. Hamdy, *European Coatings Journal*, 86, 3, (2008) 43-50.
14. H. Umehara, S. Terauchi, M. Takaya, *Mater. Sci. Forum*. 350 (2000) 273–282.
15. H. Umehara, M. Takaya, Y. Kojima, *Mater. Trans.* 42 (2001) 1691–1699.
16. K.Z. Chong, T.S. Shih, *Mater. Chem. Phys.* 80 (2003) 191–200.
17. M. Zhao, S. Wu, J. Luo, Y. Fukuda, H. Nakae, *Surf. Coat. Technol.* 200 (2006) 5407–5412.
18. F. Zucchi, A. Frignani, V. Grassi, G. Trabanelli, C. Monticelli, *Corros. Sci*. 49 (2007) 4542–4552.
19. A. S. Hamdy, *Surf. Coat. Technol*, 203 (2008), 240-249
20. A.S. Hamdy, and M. Farahat, *Surf. Coat. Technol*, 204 (2010) 2834–2840
21. A.S. Hamdy, I. Doench, and H. Möhwald, *Electrochim. Acta*, 56 (2011) 2493.
22. A.S. Hamdy, I. Doench, and H. Möhwald, *Prog. Org. Coat*., 72 (2011) 387-393
23. W. Zhou, D. Shan, E.H. Han, W. Ke, *Corros. Sci*. 50 (2008) 329–337.
24. X.B. Chen, N. Birbilis, T.B. Abbott, *Corros. Sci.* 55 (2012) 226–232.
25. T. Ishizaki, R. Kudo, T. Omi, K. Teshima, T. Sonoda, I. Shigematsu, M. Sakamoto, *Electrochim. Act*a 62 (2012) 19–29.
26. Q. Li, S. Xu, J. Hu, S. Zhang, X. Zhong, X. Yang, *Electrochim. Acta* 55 (2010) 887–894.
27. M.F. Montemor, A.M. Simones, M.J. Carmezim, *Appl. Surf. Sci.* 253 (2007) 6922–6931.
28. C.S. Lin, C.Y. Lee, W.C. Li, Y.S. Chen, G.N. Fang, *J. Electrochem. Soc*. 153 (2006) B90–B96.

29. M. Mosialek, G. Mordarsku, P. Nowak, W. Simka, G. Nawrat, M. Hanke, R.P. Socha, J. Michalska, *Surf. Coat. Technol*. 206 (2011) 51–62.
30. H. Zhang, G.C. Yao, S.L. Wang, Y.H. Liu, H.J. Luo, *Surf. Coat. Technol*. 202 (2008) 1825–1830.
31. H. Ardelean, I. Frateur, P. Marcus, *Corros. Sci.* 50 (2008) 1907–1918.
32. C. Wang, S. Zhu, F. Jiang, F. Wang, *Corros. Sci.* 51 (2009) 2916–2923.
33. E. Rocca, C. Juers, J. Steinmetz, *Corros. Sci*. 52 (2010) 2172–2178.
34. Y.C. Yang, C.Y. Tsai, Y.H. Huang, C.S. Lin, *J. Electrochem. Soc.* 159 (2012) C226–C232.
35. F. Zucchi, A. Frignani, V. Grassi, G. Trabanelli, C. Monticelli, *Corros. Sci.* 49 (2007)4542.
36. D. Hawke, D.L. Albright, *Met. Finish.* 93 (1995) 34.
37. A.S. Hamdy and H. Hussien, *Int J Electrochem Sci.*, 8 (2013) 11386 - 11402.
38. A.S. Hamdy, *European Coatings Journal*, 3 (2012), 16-20.
39. A.S. Hamdy, I. Doench, and H. Möhwald, *Surf. Coat. Technol*., 206, (2012), 3686-3692
40. A.S. Hamdy, I. Doench, and H. Möhwald, *Int J Electrochem Sci*., 7, (2012), 7751-7761.
41. W. Zhou, D. Shan, E. Han, W. Ke, *Corros. Sci*. 50 (2008) 329.
42. W.C. Neil, M. Forsyth, P.C. Howlett, C.R. Hutchinson, B.R.W. Hinton, *Corros. Sci.* 51 (2009) 387.
43. M. Zhao, S. Wu, J. Luo, Y. Fukuda, H. Nakae, *Surf. Coat. Technol.* 200 (2006) 5407.
44. K.Z. Chong, T.S. Shih, *Mater. Chem. Phys.* 80 (2003) 191.
45. H. Umehara, M. Takaya, S. Terauchi, *Surf. Coat. Technol*. 169–170 (2003) 666.
46. A.S. Hamdy and D. Butt, *Electrochim. Acta*, (2013), 296-303.